Site-Response Characteristics Evaluated from Strong Motion Records of the 2003 Boumerdes, Algeria, Earthquake

Abdelghani Meslem,[a] Fumio Yamazaki,[a] M.EERI, Yoshihisa Maruyama,[a] Djillali Benouar,[b] Nasser Laouami,[c] and Nassima Benkaci[c]

Site response characteristics at seismic stations were investigated using horizontal-to-vertical (H/V) spectral ratios calculated from a seismic-motion dataset of the 2003 Boumerdes earthquake, and transfer functions were evaluated from soil profile data. Although high peak ground acceleration (PGA) values were recorded at some sites, the nonlinear effect at these stations was not clear. The H/V spectral ratios calculated from weak and strong motion events did not show a clear difference in the predominant period and amplitudes, and the shapes of the H/V ratios were flat for some stations. These observations are characteristic of the presence of firm to hard layers under the stations; however, one station was located on Quaternary deposits showed a remarkable amplification at the predominant period and a high PGA value. [DOI: 10.1193/1.3459158]

INTRODUCTION

On 21 May 2003, at 18:44:31 (GMT), a destructive earthquake (M_w=6.8) struck the northern part of Algeria, causing extensive damage and human casualties (Ayadi et al. 2003, EERI 2003). The main shock was felt within a 250 km radius from the epicenter (Laouami et al. 2006). The location of the epicenter, as provided by the Algerian Research Center of Astronomy Astrophysics and Geophysics (CRAAG), was 36.91°N and 3.58°E. However, Bounif et al. (2004) determined that the epicenter of the main shock was at 36.83°N and 3.65°E (Figure 1), at a depth of 8–10 km. The rectangle in Figure 1 shows the focal plane projected to the surface as proposed by Delouis et al. (2004). The source model runs for an eastern distance of 55 km (3.4°–4.0°E). According to Meghraoui et al. (2004), the model fault (reverse-faulting mechanism) has a strike of N 54°E and dip of 50° to the southeast, and it extends 1–15 km below the ground surface.

Observations of recorded accelerations show a remarkable difference in maximum values among neighboring stations. However, for some stations, no such difference was observed in the velocity or acceleration for aftershocks. Local topographical and geo-

[a] Department of Urban Environment Systems, Graduate School of Engineering, Chiba University, 1-33 Yayoi-cho, Inage-ku, Chiba 263-8522, Japan
[b] Built Environment Res. Lab. (LBE), Faculty of Civil Engineering, University of Bab-Ezzouar (USTHB), BP32 El-Alia, Bab-Ezzouar, Algiers 16111, Algeria
[c] Algerian National Research Center of Earthquake Engineering (CGS), 1 Rue Kadour Rahim, Hussein-Dey, Algiers, Algeria

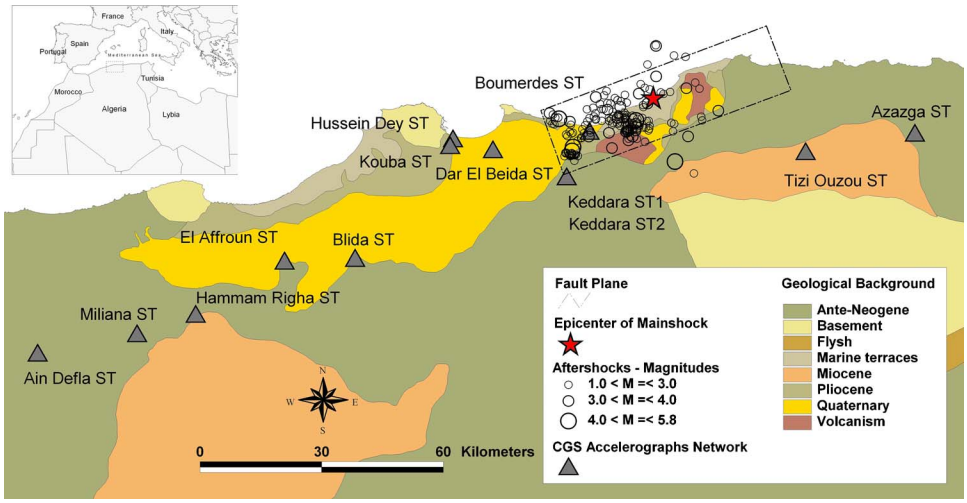

Figure 1. Geological background (Ayadi et al. 2003) of the epicentral area and the mainshock's epicenter (starred) of the 2003 Boumerdes, Algeria earthquake. The rectangle represents the estimated fault plane (reverse-faulting mechanism; Delouis et al. 2004). The graduated circles correspond to 167 aftershocks during 25-30 May 2003. The triangles represent the CGS accelerograph network stations located in the central part of northern Algeria.

logical conditions can generate significant amplifications and spatial variations in earthquake ground motions. In recent years, the horizontal-to-vertical (H/V) spectral ratio method (Nakamura 1989) has become increasingly popular in studies of site effects and determination of the predominant period of a site using earthquake records (Field and Jacob 1993, Huang and Teng 1999). In addition, observations from different parts of the world have already provided evidence of the significance of nonlinear site effects on ground-motion records (Shearer and Orcutt 1987, Beresnev et al. 1998). Several researchers have reported nonlinear site effects, which are characterized by an increase in the damping ratio and reduction in the shear wave velocity, using the spectral ratio technique (Wen 1994, Dimitriu et al. 2000, Wen et al. 2006).

In this study, we used a seismic-motion dataset of the 2003 Boumerdes earthquake, which was recorded from the Algerian Accelerograph Network and provided by the Algerian National Research Center of Earthquake Engineering (CGS), to investigate site-response characteristics through the H/V spectral ratio technique. We calculated the spectral ratios for strong and weak motion events to estimate the possibility of nonlinear site effects during earthquakes. Comparison of the calculated H/V spectral ratios with site-transfer functions obtained from existing soil profiles allowed us to examine the applicability of the H/V method regarding the expected predominant periods and amplification of soil layers under each station.

MAIN SHOCK OF THE 2003 BOUMERDES EARTHQUAKE

Historically, the northern part of Algeria has suffered from numerous seismic events (Benouar 1996). Examples of recent disastrous events include the 9 September 1954 Orleansville earthquake (M_s 6.7), which caused over 1,200 deaths and damaged over 20,000 buildings, and the 10 October 1980 El-Asnam earthquake (M_s 7.2), which caused over 2,640 deaths and damaged about 20,000 buildings. The most recent such event was the 21 May 2003 Boumerdes earthquake (M_w 6.8); the Algerian Ministers' Council (12 December 2003) reported 2,278 deaths, 11,450 injured, and an estimated 250,000 homeless, i.e., about 40,000 families (DLEP 2004). Due to building damage, 17,000 structures had to be demolished and 116,000 were repaired. The resulting direct economic loss was estimated to be US $5 billion (Ousalem and Bechtoula 2005).

The 2003 Boumerdes earthquake is the first event in Algeria for which a large number of strong motions were successfully recorded at several seismic stations by the national accelerometer network operated by CGS. This is because the countrywide accelerometer network was established only after the Algerian government established CGS following the 1980 El-Asnam earthquake (Laouami et al. 2006). Figure 1 shows the locations of 11 free-field seismic observation stations deployed by CGS, from which the main shock was recorded at a hypocentral distance of 31–165 km. However, due to some instrument problems during the event, the main shock and many aftershocks could not be recorded at some locations where the damage was most extensive.

STRONG-MOTION RECORDS

The instruments deployed by CGS record seismic ground motion using electronic transducers that produce an output voltage proportional to acceleration. Using the recorded acceleration time history, the velocity and displacement time histories are computed by integration in the frequency domain through a rectangular filter with a low cutoff frequency of 0.05 Hz. Figure 2 shows particle traces of the displacements computed from the main shock records on a horizontal plane at 11 seismic observation stations. These orbits show that the maximum displacements were recorded at Dar El-Beida ST (18.3 cm) and Hussein-Dey ST (11.4 cm). The displacement orbits at two nearby stations, Keddara ST1 and Keddara ST2, show similar shapes but appear to have a rotation angle about the vertical axis. Because the distance between two stations is very small (approximately 100 m), the observed rotation angle may be inferred as being caused by orientation errors during instrument installation. Some seismometers have been reported as being deployed with unexpected orientation errors (Yamazaki et al. 1992).

We do not know which of these two stations has the correct orientation. If we consider the orientation of the instrument at Keddara ST1 as a reference, the rotation angle at Keddara ST2 is estimated as 20.7° about the vertical axis, on the basis of the method proposed by Yamazaki et al. (1992). The orientation error of the instrument at Keddara ST2 can be corrected by rotating back the error angle. Figure 3a shows a comparison of displacements between Keddara ST1 and ST2 before and after the correction. Displacement time histories for Keddara ST1 and ST2 became very similar after the correction,

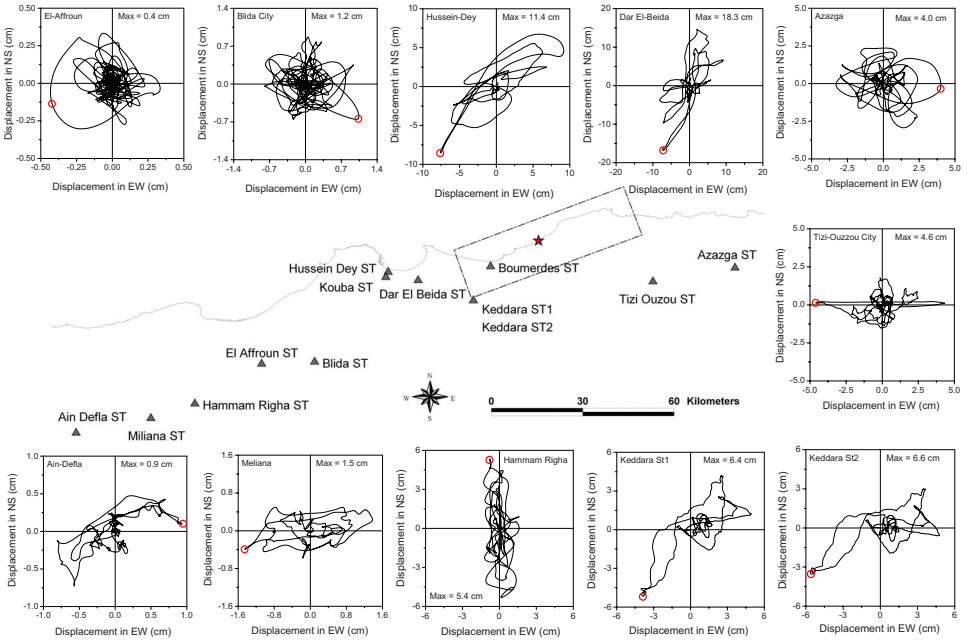

Figure 2. Orbit plots of displacement computed from the recorded mainshock for 11 seismic stations. The open circles correspond to the direction of the maximum resultant value.

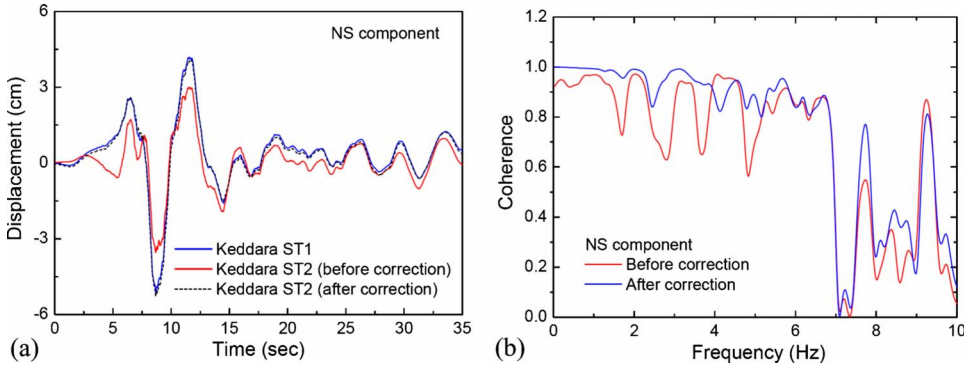

Figure 3. Comparison of (a) displacements and (b) coherence functions between Keddara ST1 and Keddara ST2 before and after the orientation-error correction.

Table 1. Peak ground acceleration, velocity, and displacement corresponding to the resultant of the horizontal components for the mainshock of the 2003 Boumerdes earthquake, and the instrumental JMA intensity and estimated MMI. The EMS-98 intensity was estimated following the macroseimic survey conducted by CRAAG.

Station	Location	Hypocentral Distance (km)	PGA (cm/s^2)	PGV (cm/s)	PGD (cm)	JMA	MMI	EMS-98
Boumerdes	36.75 N 03.47 E	21	—	—	—	—	—	X
Keddara ST1	36.65 N 03.41 E	31	333.0	18.5	6.4	4.7	VII	VII
Keddara ST2	36.65 N 03.41 E	31	580.5	19.8	6.6	4.8	VII	VII
Tizi Ouzou	36.70 N 04.07 E	41	231.7	13.9	4.6	4.4	VI	VI
Dar El-Beida	36.71 N 03.20 E	43	540.0	41.9	18.3	5.6	VIII	VIII
Hussein Dey	36.74 N 03.09 E	52	272.0	20.1	11.4	4.8	VII	VI-VII
Kouba	36.71 N 03.09 E	53	—	—	—	—	—	VI
Azazga	36.74 N 04.37 E	66	120.5	14.8	4.0	4.6	VI	VI
Blida	36.47 N 02.82 E	85	52.3	3.6	1.2	3.6	V	V
El Affroun	36.47 N 02.63 E	100	164.4	5.6	0.4	4.2	V	V
Hammam Righa	36.35 N 02.39 E	125	114.8	14.0	5.4	4.6	VI	IV
Miliana	36.30 N 02.23 E	140	34.2	2.4	1.5	3.3	IV	IV
Ain Defla	36.26 N 01.95 E	165	36.1	1.8	0.9	3.1	IV	IV

while they were clearly different before the correction. The corresponding coherence functions are shown in Figure 3b. Coherence increased after the correction.

Thus, when two stations are located close to each other, we can calculate their orientation errors; however, it is difficult to do so for stand-alone stations. Hence, in this study, the resultant A_{res} of the two horizontal components (Ansary et al. 1995) was used to eliminate or avoid the possibility of orientation error.

$$A_{res}(t) = \sqrt{A_{NS}(t)^2 + A_{EW}(t)^2} \tag{1}$$

Table 1 shows the recorded peak ground acceleration (PGA) with the computed peak ground velocity (PGV) and peak ground displacement (PGD) corresponding to the

maximum values resulting from two horizontal components (NS and EW). The largest PGA values were recorded at Keddara ST2 (580.5 cm/s^2) and Dar El-Beida station (540.0 cm/s^2). The PGAs for some of the stations differed greatly from those of neighboring stations, but the PGVs and PGDs for other stations showed no such difference. Although a considerable difference was seen in the PGAs for Keddara ST1 (330.0 cm/s^2) and the nearby Keddara ST2, the PGV (18.5 and 19.8 cm/s, respectively) and PGD values (6.4 and 6.6 cm, respectively) were very close. Acceleration is well known to be sensitive to high-frequency content, but the velocity and displacement are much less so. Hence, the big difference in PGA and small differences in PGV and PGD are due to the high-frequency content of seismic motion.

SEISMIC INTENSITY

The Modified Mercalli Intensity (MMI) scale (Wood and Neumann 1931), European Macroseismic Scale (EMS-98) (Grünthal 2001), and Japan Meteorological Agency (JMA) scale (Karim and Yamazaki 2002), developed in the USA, Europe, and Japan, respectively, are among the most widely used to estimate the ground motion severity. The MMI and EMS-98 generally estimate the ground shaking intensity during an earthquake using scales based on the effects felt at the time of the earthquake and on later observations of damage to the built environment. Twelve grades denoted by the Roman numerals I–XII are defined. Each degree in these scales describes the effects of ground motion on nature or the built environment in terms of damage, ranging from I, denoting a weak earthquake motion, to XII, denoting almost total destruction. Recently, the estimation of MMI intensity has been related, to the ground motion records (Wald et al. 1999a and 1999b), where the scale of MMI intensity can be estimated according to the value ranges of peak ground motions recorded at a seismic station.

In contrast, the JMA scale is based on strong-motion records. Although the JMA intensity scale is initially based on the intensity felt with eight shaking levels, it was later revised to allow the use of seismic intensity computed from strong-motion records. The computation of JMA intensity (also denoted as I_{JMA}) involves combining the three components of recorded motion; the numerical seismic intensity value is determined from the acceleration value a_0 that persists for a sufficient duration (Shabestari and Yamazaki 2001).

$$I_{JMA} = 2.01\ log(a_0) + 0.94 \tag{2}$$

In this study, JMA and MMI intensity scales were applied to mainshock records obtained during the 2003 Boumerdes earthquake. The computed JMA intensities ranged from 3.1 to 5.6, as shown in Table 1. The maximum value was obtained at Dar El-Beida station, about 43 km from the hypocenter. For the two stations, Keddara ST1 and Keddara ST2, the JMA intensity values were similar at 4.7 and 4.8, respectively. The estimated MMI intensities for the mainshock records at their corresponding seismic stations are also shown by Table 1.

In addition, the EMS-98 intensity scale was applied to the 2003 Boumerdes earthquake (Harbi et al. 2007) following the macroseismic survey conducted by CRAAG. The EMS-98 intensity was estimated for 600 sites. The maximum attributed intensities IX

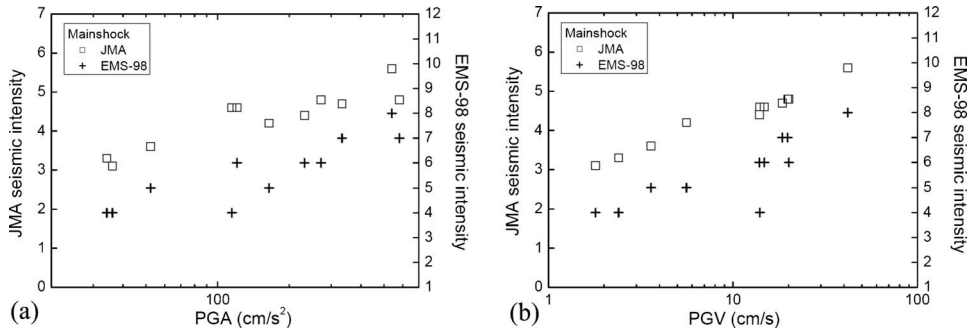

Figure 4. Comparison of JMA and EMS-98 seismic intensities using (a) PGA and (b) PGV for the mainshock records.

and X were assigned to 11 sites, where many constructions suffered heavy to very heavy damage or collapse. An intensity of VIII was assigned to 22 sites where damage to buildings and loss of life were recorded. As shown in Table 1, we associated each strong-motion record obtained from the free-field recording sites with the EMS-98 value assigned to where the strong motion was recorded and felt by people.

As shown in Table 1, almost all of the estimated MMI intensity grades matched quite well with the EMS-98 intensities. Figure 4 shows a comparison of JMA and EMS-98 intensities with the peak ground motions of the mainshock. The correlation of PGA to EMS-98 is clearly not as good as the correlation of the latter to JMA.

GROUND RESPONSE ANALYSIS

SELECTED SEISMIC STATIONS

To examine the local site effects of recorded strong motions of the 2003 Boumerdes, Algeria earthquake, six near-field seismic stations were selected: Hussein-Dey, Kouba, Dar El-Beida, Boumerdes, Keddara ST1, and Keddara ST2. All of these stations are located approximately along the fault trace (Figure 1). The average distance between adjacent stations is about 20.4 km. According to the geological background (Ayadi et al. 2003) shown in Figure 1, the area where these stations are located is comprises mainly of Quaternary and Neogene formations. Quaternary formations, which are generally soft deposits, consist of mostly sand, gravel, and sandy clay covering Plaisancian (lower Pliocene) blue marl and Cristallophyllian rocks; they extend to 30 m beneath the ground surface.

At Hussein-Dey and Kouba cities, old masonry residential buildings built before 1960, an example of which is shown in Figure 5a, were the most affected by the mainshock. The recorded mainshock at Hussein-Dey ST had PGA=272.0 cm/s^2 and PGV =20.1 cm/s (Table 1), which corresponds to I_{JMA}=4.8 and EMS-98=VI–VII. These intensities were at the lower limit at which structural damage starts to occur to vulnerable buildings. For Dar El-Beida city, the mainshock caused heavy damage with I_{JMA}=5.6 and EMS-98=VIII. Damaged buildings tended to be made of reinforced concrete as well as old

Figure 5. Typical damaged buildings in the area of study. (a) Exterior wall collapse of a 6-storied old masonry building (EMS-98=VI) located in a dense urban area, not far from Hussein-Dey ST. (b) Collapse of the first and second floors of a 5-storied RC building (EMS-98 =X) 600 m away from the Boumerdes ST.

masonry. In Boumerdes city, the mainshock was particularly destructive with EMS-98=X. Many constructions, mostly mid-rise reinforced concrete buildings (4 and 5 stories) built after 1970 (Figure 5b), were destroyed, and many people were killed as a result of the destruction of buildings. For Keddara ST1 and ST2, located 13 km away from Boumerdes city, the JMA intensities of the mainshock were 4.7 and 4.8, respectively, with an estimated EMS-98=VII. Note that the two neighboring stations are located in a mountain basin; an earth dam was located only 700 m away from the two stations.

The mainshock of the 21 May 2003 event was followed by many aftershocks, some of them with magnitudes over 5.0. A total of 167 aftershocks were recorded from 25 May to 30 May 2003, as shown in Figure 1. From the six selected seismic recording stations, 239 seismic events (mainshock and aftershocks) were recorded: 89 from Boumerdes, 47 from Keddara ST2, 34 from Keddara ST1, 28 from Kouba, 27 from Dar El-Beida, and 14 from Hussein-Dey. Figure 6 shows the levels of all recorded PGA and PGV for the six stations. Strong aftershocks were mostly observed at Boumerdes, Dar El-Beida, and Keddara. The largest aftershock record was obtained at Boumerdes (M =5.8, on 27 May 2003 at 17:11:40 GTM at 36.78°N and 3.60°E), with PGA =441.5 cm/s^2 and PGV=23.59 cm/s. Table 2 shows details of 14 selected seismic records (with a sufficient record length) from each of the six stations: one record from the mainshock and 13 records from aftershocks. However, only aftershock records for Boumerdes and Kouba were selected because the mainshock could not be recorded.

H/V SPECTRAL RATIOS

Aiming to estimate local site-response characteristics, Nakamura (1989) proposed the well-known H/V spectral ratio technique, which uses the ratio of horizontal and vertical Fourier spectra of microtremors recorded at a site. Several researchers have attempted to apply the technique to earthquake records (Yamazaki and Ansary 1997). In general, the H/V spectral ratio is used to estimate the predominant period (peak period of the H/V ratio), which is used as a significant parameter in building damage assessment (Fallahi et al. 2003, Gosar 2007) and in estimating soil amplification characteristics

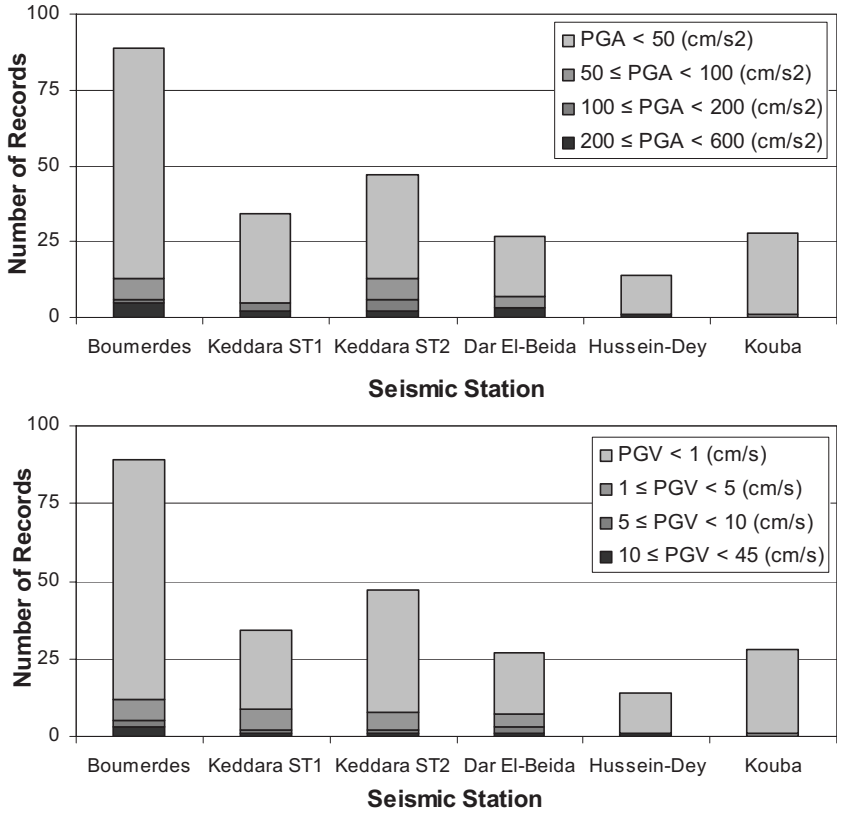

Figure 6. Number of recorded ground motions and range of PGV and PGA values at six seismic stations.

(Rodriguez and Midorikawa 2003). In recent years, studies have demonstrated that nonlinear behavior (shear-modulus degradation) can be evaluated using H/V spectral ratios. When nonlinearity occurs in a soil layer under a seismic station, the predominant period is lengthened accordingly (Wen 1994, Wen et al. 2006). The nonlinear effect is evidenced through an increase in the predominant period of soil deposits with an increasing level of excitation (Beresnev et al. 1998, Huang 2002).

We calculated the H/V Fourier spectral ratio for all seismic records used in this study as the spectral ratio between the two horizontal components (EW and NS) and vertical (UD) component, defined by

$$R(f) = \frac{\sqrt{F_{NS}(f) \cdot F_{EW}(f)}}{F_{UD}(f)} \tag{3}$$

where $F_{NS}(f)$, $F_{EW}(f)$, and $F_{UD}(f)$ are the smoothed Fourier-amplitude spectra for the two horizontal and vertical components of a seismic-motion record, respectively. These Fourier

Table 2. Resultant peak horizontal acceleration and velocity for 14 seismic records for the 2003 Boumerdes earthquake

Boumerdes ST				Dar El-Beida ST			
Date	Time (GMT)	PGA (cm/s^2)	PGV (cm/s)	Date	Time (GMT)	PGA (cm/s^2)	PGV (cm/s)
27/05/2003	17:11:40	441.5	23.59	21/05/2003	18:44:31	539.97	41.89
28/05/2003	06:36:59 (*)	4.64	0.06	27/05/2003	18:06:13 (*)	2.21	0.04
28/05/2003	14:41:18 (*)	5.97	0.07	28/05/2003	06:58:44	396.02	8.67
28/05/2003	17:01:40	2.93	0.05	28/05/2003	11:26:27 (*)	7.71	0.18
28/05/2003	17:02:40	2.44	0.03	28/05/2003	14:41:18	3.12	0.06
29/05/2003	02:15:07	310.9	12.23	28/05/2003	19:05:31 (*)	9.16	0.30
29/05/2003	02:21:55 (*)	73.1	1.16	29/05/2003	02:15:07	251.97	7.31
01/06/2003	09:00:48	37.13	0.58	29/05/2003	02:21:55	58.43	0.94
01/06/2003	22:54:32 (*)	52.95	1.29	02/06/2003	22:31:05 (*)	39.67	0.85
03/08/2003	09:56:52 (*)	40.33	0.8	05/06/2003	21:54:44	26.71	0.21
11/08/2003	20:03:53	126	2.44	16/10/2003	06:38:16	99.56	1.70
19/09/2003	14:11:56 (*)	35.15	0.34	19/10/2003	04:52:23	71.00	1.29
10/01/2004	18:38:15	575.5	16.75	10/01/2004	18:38:15 (*)	45.81	1.75
05/12/2004	08:31:24	413.9	8.77	01/12/2004	17:42:49 (*)	85.76	1.83

(*): records considered for computing the average of H/V for weak seismic motions in Figure 10.

Hussein-Dey ST				Kouba ST			
Date	Time (GMT)	PGA (cm/s^2)	PGV (cm/s)	Date	Time (GMT)	PGA (cm/s^2)	PGV (cm/s)
21/05/2003	18:44:31	272.01	20.10	28/05/2003	19:05:31	6.77	0.20
12/10/2003	07:08:00 (*)	3.70	0.12	29/05/2003	02:15:07 (*)	78.63	2.57
16/10/2003	06:38:16 (*)	6.83	0.16	29/05/2003	02:21:55 (*)	16.17	0.40
19/10/2003	04:52:23	9.15	0.14	29/05/2003	05:03:07 (*)	4.22	0.07
11/11/2003	17:47:36 (*)	2.12	0.06	29/05/2003	09:58:17 (*)	1.88	0.05
15/11/2003	16:31:52	4.43	0.05	29/05/2003	19:43:20 (*)	8.64	0.19
12/12/2003	01:35:53	1.54	0.04	31/05/2003	11:44:58	1.96	0.06
13/12/2003	07:03:36 (*)	1.56	0.04	01/06/2003	06:07:35	1.93	0.06
13/12/2003	16:07:39	1.83	0.05	02/06/2003	08:20:25	3.03	0.07
02/01/2004	07:23:12	7.48	0.01	02/06/2003	22:31:05	9.22	0.23
10/01/2004	18:38:15	20.96	0.58	04/06/2003	08:10:50	6.83	0.16
13/09/2004	13:33:56	1.55	0.03	05/06/2003	21:54:44 (*)	3.26	0.07
01/12/2004	17:42:49 (*)	5.51	0.21	06/06/2003	00:04:46	2.11	0.05
05/12/2004	08:31:24 (*)	9.10	0.18	06/06/2003	03:13:57	2.76	0.10

(*): records considered for computing the average of H/V for weak seismic motions in Figure 10.

		Keddara ST1		Keddara ST2	
Date	Time (GMT)	PGA (cm/s^2)	PGV (cm/s)	PGA (cm/s^2)	PGV (cm/s)
21/05/2003	18:44:31	332.95	18.51	580.45	19.75
26/05/2003	16:01:30	26.29	0.64	31.27	0.53
27/05/2003	17:11:40	123.80	4.38	150.33	4.22
28/05/2003	06:58:44	49.60	1.31	104.90	1.48
29/05/2003	02:15:07	225.27	5.89	365.07	5.93
29/05/2003	02:21:55	36.27	0.60	43.94	0.75
11/06/2003	17:28:34	1.60	0.03	1.90	0.03
14/06/2003	15:23:30	2.08	0.03	3.44	0.03
15/06/2003	11:01:52	5.50	0.06	10.40	0.08
18/06/2003	19:36:11	1.81	0.04	2.24	0.04
19/06/2003	10:08:14	2.75	0.05	2.90	0.04
14/07/2003	22:52:21	23.59	0.63	35.29	0.65
16/06/2004	17:29:16	28.20	0.42	54.34	0.72
05/12/2004	08:31:24	33.11	1.12	63.19	1.15

spectra were smoothed by a Parzen window of 0.4 Hz bandwidth. Figure 7 shows examples of the H/V spectral ratios for six stations using three seismic records (see Table 2) with different excitation levels (PGV levels). The H/V spectral ratio for an earthquake ground motion appeared to be influenced by the site characteristics, which correlates well with the fact that the H/V spectral ratio is sensitive to ground-motion intensity (Dimitriu et al. 2000).

In general, each station had similar shapes for the H/V spectral ratios, with no clear difference in amplitude for differing PGV levels of seismic motion. The shapes of the ratios showed the presence of noise, including fluctuation around the expected predominant period, which is defined as the period at which the maximum soil amplification occurs (Fellahi et al. 2003). These peaks were observed at the Boumerdes, Dar El-Beida, Kouba, and Hussein-Dey stations. In contrast to these stations, the two neighboring stations Keddara ST1 and ST2, which were only separated by about 100 m, exhibited H/V ratios with an almost flat form and no particular difference in the shape between them except for the presence of a small peak around 0.10–0.15 s in Keddara ST1; this peak was unclear according to the criteria defined by SESAME project (SESAME 2004) for reliable and clear peaks.

For selected stations, the evidence of soil nonlinearity from the H/V spectral ratios for different PGV levels is not clear; the small shifts in peaks shown in Figure 7 are almost negligible. From literature, when the H/V-ratio technique is used, the predominant period should correspond to the highest peak amplitude of a H/V curve (Oliveira et al. 2006). Hence, for each event, we estimated the predominant period from the computed H/V spectral ratio. Figure 8 shows the extracted predominant periods from the H/V spectral ratio for 14 seismic motions with respect to PGV. The results from all of

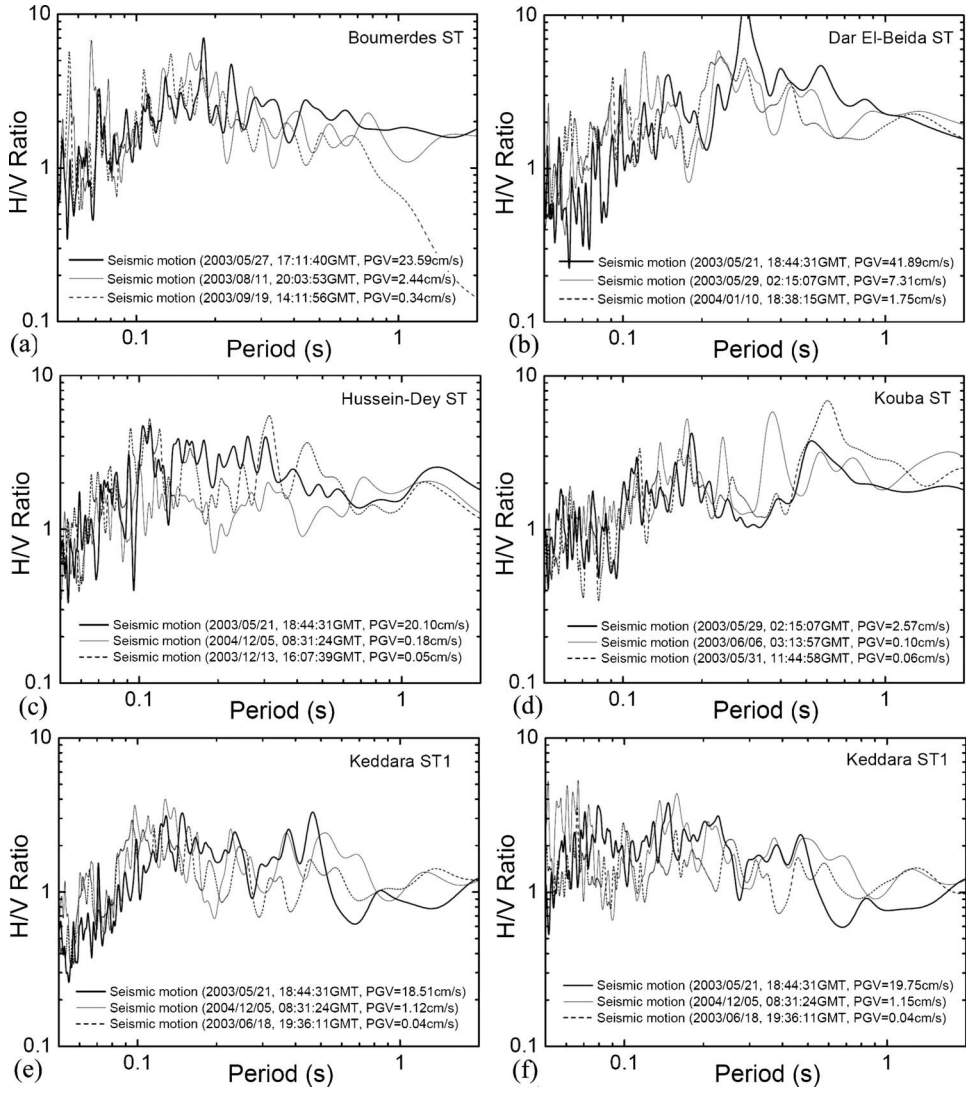

Figure 7. Comparison of the H/V spectral ratios among strong and weak seismic motions at six seismic stations: (a) Boumerdes, (b) Dar El-Beida, (c) Hussein-Dey, (d) Kouba, (e) Keddara ST1, and (f) Keddara ST2.

the stations do not present convincing evidence of an increase in the predominant period with the motion intensity. Only two stations, Boumerdes and Dar El-Beida, showed even slight increases, which seems insignificant (Figure 8).

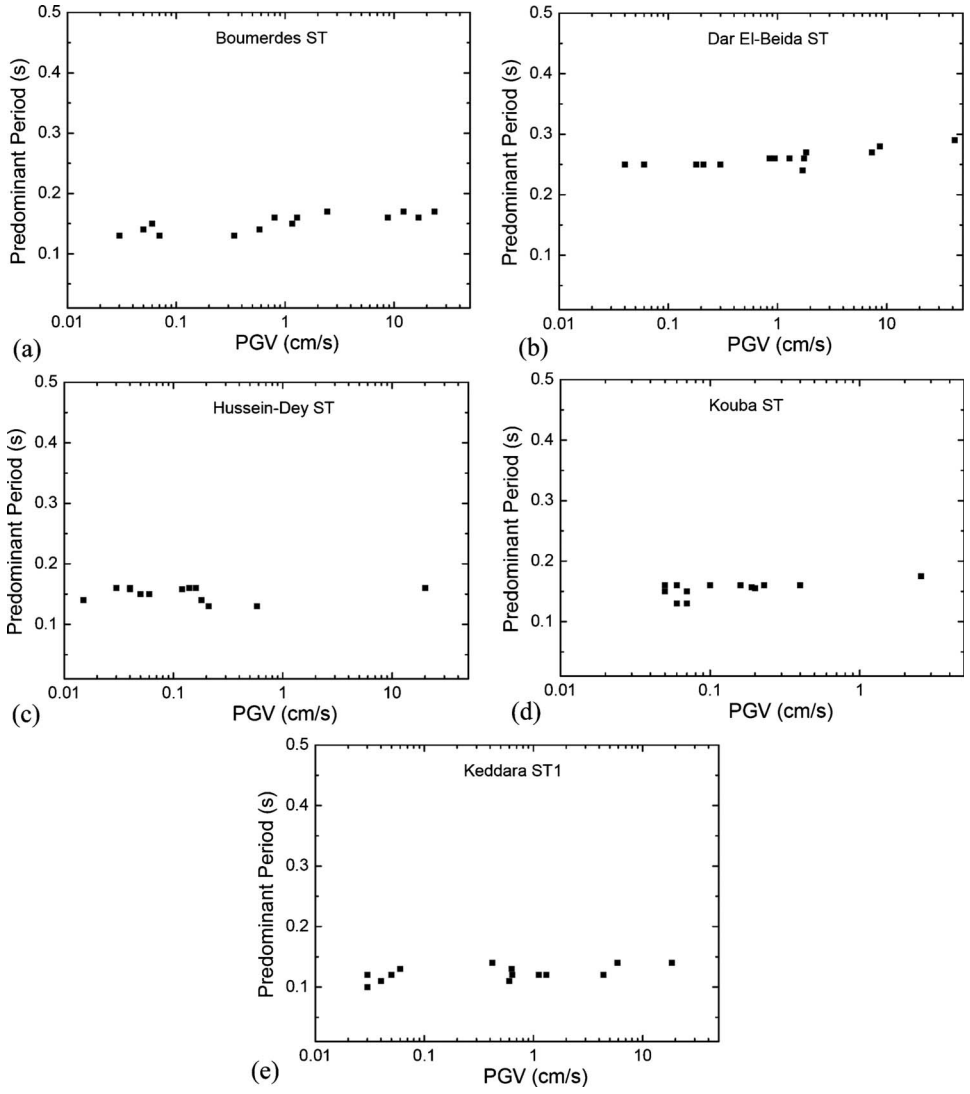

Figure 8. Predominant periods of the H/V spectral ratios with respect to PGV (Table 2) at five seismic stations: (a) Boumerdes, (b) Dar El-Beida, (c) Hussein-Dey, (d) Kouba, and (e) Keddara ST1.

COMPARISON BETWEEN THE H/V SPECTRAL RATIO AND TRANSFER FUNCTION

Out of the six seismic stations, detailed soil profiles are only available for four (Figure 9): Hussein-Dey (up to −58 m), Kouba (up to −40 m), Dar El-Beida (up to −60 m), and Boumerdes (up to −25 m). Shear-wave (S-wave) velocity profiles are only available for two stations, Hussein-Dey and Kouba, and were obtained from in situ downhole measure-

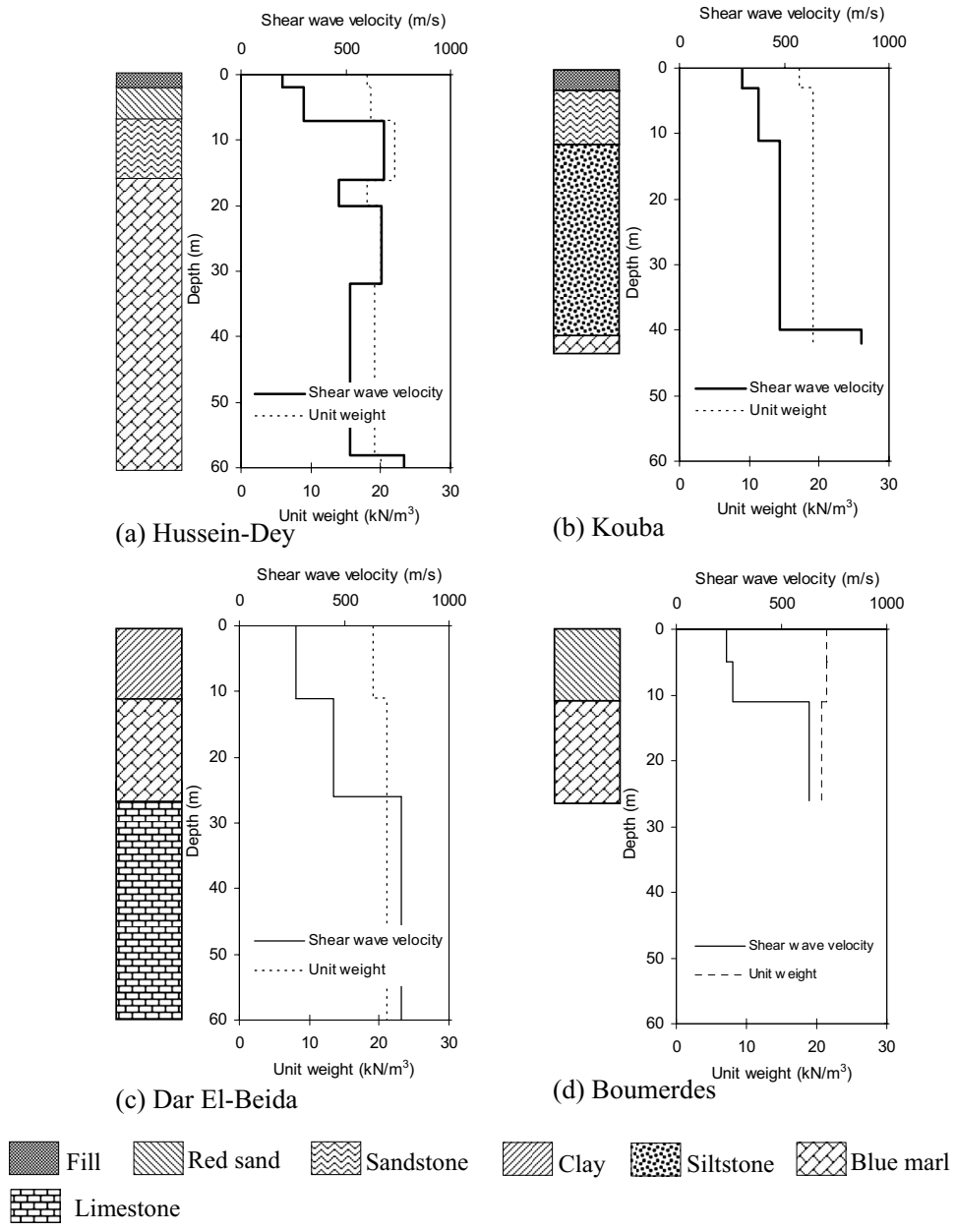

Figure 9. Soil classifications and S-wave velocity profiles for four seismic stations in Algiers and Boumerdes provinces. (a) and (b): The measured S-wave velocity (thick line) was measured by a downhole survey. (c) and (d): The estimated S-wave velocity (thin line) used existing engineering classification models for different geological units in these areas (JICA and CGS 2006).

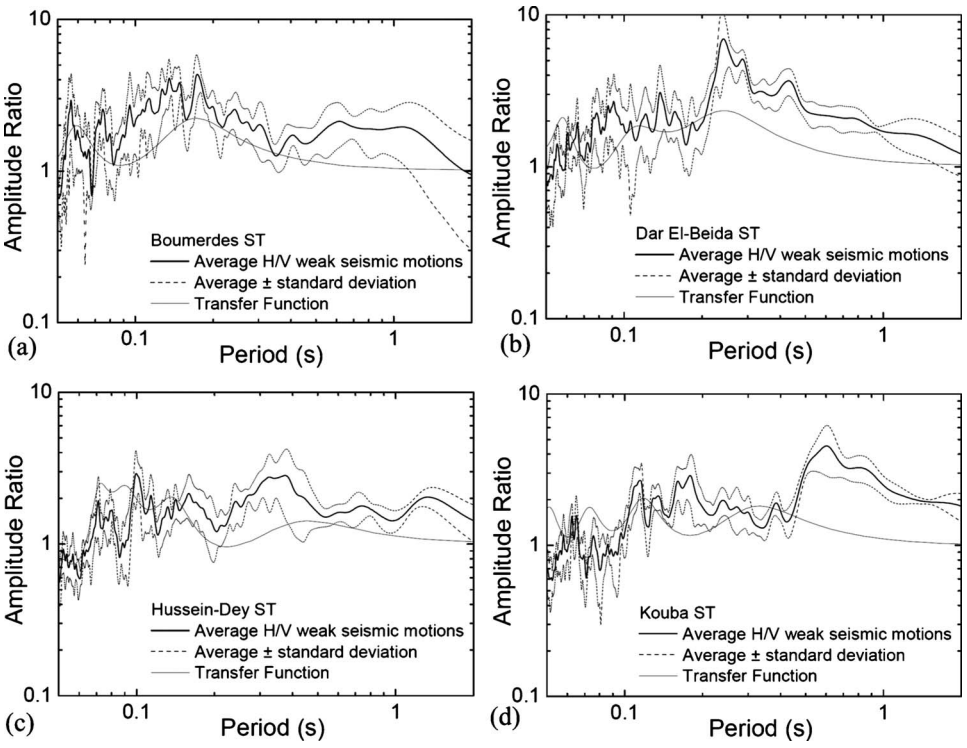

Figure 10. Average of the six selected H/V spectral ratios for weak seismic motions (thick black line) versus the transfer function (thin black line) at four seismic stations: (a) Boumerdes, (b) Dar El-Beida, (c) Hussein-Dey, and (d) Kouba. The dashed line shows the plus-minus one standard deviation range of the averaged H/V ratio.

ments. For Dar El-Beida and Boumerdes, generalized S-wave velocity profiles were estimated using the standard S-wave velocity with respect to geological layers; these were proposed for Algiers province by the Japan International Cooperation Agency (JICA) in cooperation with CGS (JICA and CGS 2006).

The transfer function, defined as the ratio of the surface motion with respect to the rock outcrop motion, was calculated for four stations using the computer program SHAKE91 (Idriss and Sun 1992). The behavior of soil sites was considered linear assuming that the shear wave velocity and damping did not change. Damping ratios of 2% for different soil layers and 1% for bedrock (outcrop) were used to compute the transfer function. Figure 10 compares the average H/V spectral ratio (Field and Jacob 1995) with the transfer function for the Boumerdes, Dar El-Beida, Hussein-Dey, and Kouba stations. Since PGV levels may be relevant for soil nonlinearity, the average for the H/V spectral ratios, which may reduce uncertainty (Aki and Richards 1980), was computed using six weak motion records, i.e., using similar levels of excitation without nonlinearity. The selected records for averaging are denoted in Table 2 by asterisks.

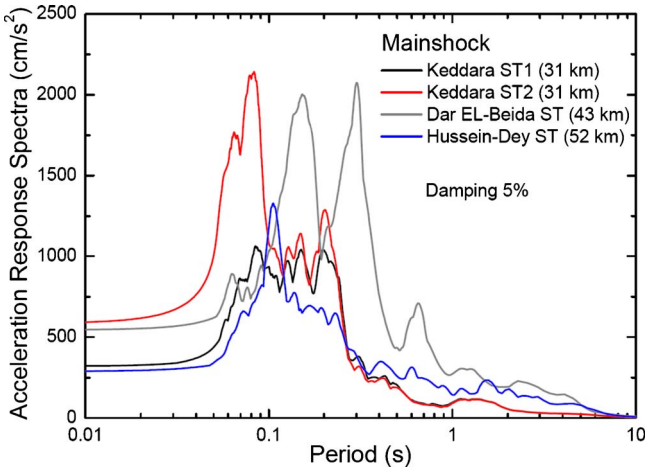

Figure 11. Resultant acceleration response spectra (5% damping) for the horizontal components of the mainshock at Dar El-Beida ST, Hussein-Dey ST, Keddara ST1, and ST2.

In general, the H/V spectral ratio was reliable in characterizing the site response of soil deposits under a seismic station. The shapes of the averaged H/V ratio matched well with that of the transfer function for each site. Almost all of the predominant periods, corresponding to the maximum peak of the transfer function for a subsoil model, matched the closest peaks from the H/V ratios at the respective sites. However, the fluctuation around these peak periods from the averaged H/V ratios was rather significant for Hussein-Dey and Kouba (Figure 10).

DISCUSSION

SITE AMPLIFICATION EFFECTS

Several authors have shown that building damage is dependant on the proximity between the natural period of a building and the predominant period of the site (Oliveira et al. 2006). Since the period range of an ordinary site is less than 1 s, the expected predominant periods (highest peak of the H/V spectral ratio) for the ground surface at the seismic stations were about 0.1–0.25 s (Figure 7 and 10).

For the Hussein-Dey and Kouba stations, which are 3 km apart, the shapes of the H/V spectral ratio did not show any significant amplification. The response spectra of the recorded mainshock at Hussein-Dey for a damping ratio of 5% (Figure 11) showed a maximum response acceleration at a period of about 0.1 s.

According to the H/V spectral ratios, the ground motion at Dar El-Beida station seems to have been strongly affected by the local soil conditions, with remarkable amplification around 0.22 s. The response spectra for Dar El-Beida, shown in Figure 11, had

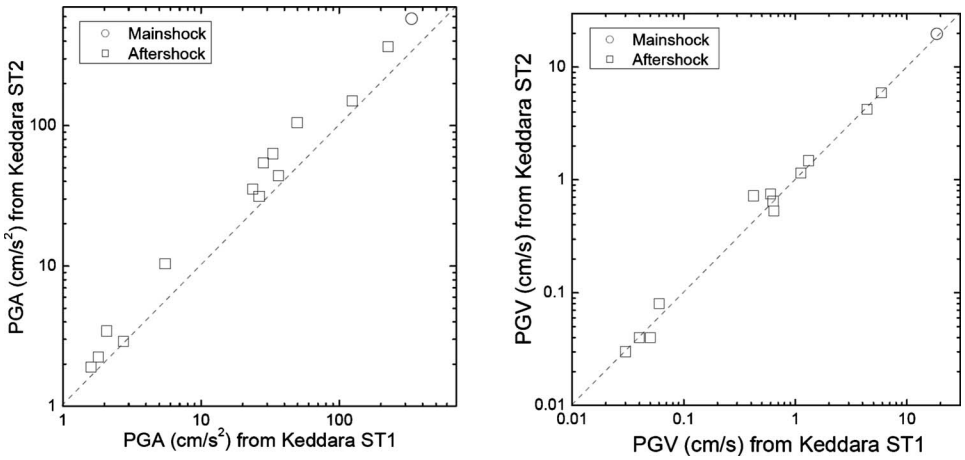

Figure 12. Comparison of PGAs and PGVs between Keddara ST1 and Keddara ST2 for the mainshock and aftershocks.

two large peaks at 0.15 and 0.3 s. Quaternary deposits are known to cover almost the entire area of this city (Figure 1), and this soil condition may be responsible for the amplification around 0.15–0.3 s.

At Boumerdes station, the H/V spectral ratios did not show any significant amplification, and the estimated predominant period of the site was around 0.15 s. As mentioned earlier, the mainshock was not recorded at this station; however, many strong aftershocks were recorded. This city is located just above the source plane; thus, the ground motion was very intense, and the observed damage was very extensive (Figure 5b).

For the two neighboring stations Keddara ST1 and ST2, which were located at the southwest edge of the strong shaking zone, the shapes of the H/V spectral ratios for seismic motions showed a similar flat form corresponding to the existence of hard surface layers, with an insignificant difference occurring at the short period around 0.11 s at Keddara ST1. Figure 12 shows a comparison for the PGA and PGV of the mainshock and aftershocks between Keddara ST1 and ST2. Most of the events clearly had similar values for the two stations, although the response spectra of the mainshock for Keddara ST1 was relatively flat compared to that for Keddara ST2, which showed a higher amplitude at 0.08 s (Figure 11). High-frequency content in seismic ground motion is well known to contribute significantly to the maximum values (Kramer 1996, Rathje et al. 2004). This observation suggests the need for detailed geotechnical data to investigate the reason for this difference in more detail.

NONLINEAR SITE EFFECTS

The observation of significant nonlinearity effect depends on the existence of resonance, which is related to the properties of soil deposits. Dimitriu et al. (1999) used the HV spectral ratio technique to observe a considerable drop in the effective resonance

frequency of a soil site with simple geology at the town of Lefkas in western Greece and linked it to nonlinear behavior (shear-modulus degradation) of the top sandy-silt layer. Furthermore, they found a significant correlation between the resonance frequency and PGA and PGV.

For the selected stations in this study, we did not register evidence of significant nonlinear site effects. Except for Dar El-Beida station, the H/V spectral ratios were not dominated by a clear period; moreover, the two close stations, Keddara ST1 and ST2, showed flat H/V curves (Figure 7). The shift of the dominant period from the H/V ratio was almost negligible (Figure 8); thus, we can say that the nonlinear soil effects were not so significant. In general, this characterizes the case for the presence of firm or hard soil conditions (Wen et al. 2006). With nonlinear effects, strong motions are generally less amplified than weak motions in the H/V spectral ratio (Dimitriu et al. 2000), which was not clearly seen for this study (Figure 7) throughout the range of the period.

CONCLUSION

This study analyzed the site response of accelerograph stations and the recorded strong-motion distribution during and following the 2003 Boumerdes, Algeria earthquake. The H/V spectral ratios between strong and weak motion events were compared with the aim of estimating the nonlinear site response during the earthquake. The averaged H/V spectral ratio was calculated and compared with the transfer function; it was computed using a soil layer model for each station to examine the applicability of the H/V technique regarding the predominant period and soil amplification of each station.

For the selected six stations, no significant nonlinear site effect was observed. Almost no remarkable difference in the H/V ratio was seen between the weak and strong events. The H/V ratio showed a rather flat form for some stations; hence, the predominant period was not very easy to determine in some cases. This observation suggests the presence of firm to hard soil layers under the stations, except for one station—Dar El-Beida—that showed a remarkable amplification at the predominant period, which seems to agree well with the known geological nature of the site and justifies the recorded high PGA.

This study validates the use of the H/V ratio technique to evaluate site response characteristics. However, geotechnical and geophysical investigations are needed to understand site amplification in greater detail.

ACKNOWLEDGMENTS

We express our sincere gratitude to three anonymous reviewers for their valuable contributions, suggestions, and comments in improving the scientific quality of this paper. The ground motion data used in this study were provided by the Algerian National Research Center of Earthquake Engineering (CGS).

REFERENCES

Aki, K., and Richards, P. G., 1980. *Quantitative Seismology, Theory and Methods*, W. H. Freeman, San Francisco, 558 pp.

Ansary, M. A., Yamazaki, F., and Katayama, T., 1995. Statistical analysis of peaks and directivity of earthquake ground motion, *Earthquake Eng. Struct. Dyn.* **24**, 1527–1539.

Ayadi, A., Maouche, S., Harbi, A., Meghraoui, M., Beldjoudi, H., Oussadou, F., Mahsas, A., Benouar, D., Heddar, A., Rouchiche, Y., Kherroubi, A., Frogneux, M., Lammali, K., Benhamouda, F., Sebai, A., Bourouis, S., Alasset, P. J., Aoudia, A., Cakir, Z., Merahi, M., Nouar, O., Yelles, A., Bellik, A., Briole, P., Charade, O., Thouvenot, F., Semane, F., Ferkoul, A., Deramchi, A., and Haned, S. A., 2003. Strong Algerian earthquake strikes near capital city, *EOS Trans. Am. Geophys. Union* **84**, 561–568.

Benouar, D., 1996. Seismic hazard evaluation of Algiers using Benouar's earthquake catalogue, *Natural Hazards* **13**, 119–131.

Beresnev, I. A., Field, E. H., Van Den Abeele, K., and Johnson, P. A., 1998. Magnitude of nonlinear sediment response in Los Angeles basin during the 1994 Northridge, California, earthquake, *Bull. Seismol. Soc. Am.* **88**, 1079–1084.

Bounif, A., Dorbath, C., Ayadi, A., Meghraoui, M., Beldjoudi, H., Laouami, N., Frogneux, M., Slimani, A., Kharroubi, A., Ousadou, F., Chikh, M., Harbi, A., Larbes, S., and Maouche, S., 2004. The 21 May 2003 Zemmouri (Algeria) earthquake M_w 6.8: Relocation and aftershock sequence analysis, *Geophys. Res. Lett.* **31**, L19606 doi:

Delouis, B., Vallee, M. Meghraoui, Calais, E., Maouche, S., Lammali, K., Mahras, A., Briole, P., Benhamouda, F., and Yelles, K., 2004. Slip distribution of the 2003 Boumerdes-Zemmouri earthquake, Algeria, from teleseismic, GPS, and coastal uplift data, *Geophys. Res. Lett.* **31**, L18607 doi:

Direction du Logement et des Equipements Publics de la Wilaya de Boumerdes (DLEP), 2004. *Conséquences du séisme sur le parc logement et les équipements publics*, Direction du Logement et des Equipements Publics de la Wilaya de Boumerdes.

Dimitriu, P., Kalogeras, I., and Theodulidis, N., 1999. Evidence of nonlinear site response in horizontal-to-vertical spectral ratio from near-field earthquake, *Soil Dyn. Earthquake Eng.* **18**, 423–435.

Dimitriu, P., Theodulidis, N., and Bard, P.-Y., 2000. Evidence of nonlinear site response in HVSR from SMART1 (Taiwan) data, *Soil Dyn. Earthquake Eng.* **20**, 155–165.

Earthquake Engineering Research Institute (EERI), 2003. *The Boumerdes, Algeria, Earthquake of 21 May 2003*, Reconnaissance Report, Learning from Earthquakes Program, Oakland, CA.

Fellahi, A., Alaghebandian, R., and Miyajima, M., 2003. Microtremor measurements and building damage during the Changureh-Avaj, Iran, earthquake of June 2002, *J. Nat. Disaster Sci.* **25**, 37–46.

Field, E. H., and Jacob, K. H., 1993. The theoretical response of sedimentary layers to ambient seismic noise, *Journal Geophysical Research Letters* **20**, 2925–2928.

——, and Jacob, K. H., 1995. A comparison and test of various site response estimation techniques, including three that are non reference-site dependent, *Bull. Seismol. Soc. Am.* **85**, 1127–1143.

Gosar, A., 2007. Microtremor HVSR study for assessing site effects in the Bovec Basin (NW

Slovenia) related to 1998 M_w 5.6 and 2004 M_w 5.2 earthquakes, *Engineering Geology* **91**, 178–193.

Grünthal, G., 2001. European Microseismic Scale 1998, *Cahiers du Centre Européen de Géodynamique et de Séismologie* **19**, 103.

Harbi, A., Maouche, S., Ousadou, F., Rouchiche, Y., Yelles-Chaouche, A., Merahi, M., Heddar, A., Nouar, O., Kherroubi, A., Beldjoudi, H., Ayadi, A., and Benouar, D., 2007. Macroseismic study of the Zemmouri earthquake of 21 May 2003 (M_w 6.8, Algeria), *Earthquake Spectra* **23**, 315–332.

Huang, H. C., and Teng, T. L., 1999. An evaluation on H/V ratio vs spectral ratio for site response estimation using the 1994 Northridge earthquake sequence, *Pure Appl. Geophys.* **156**, 631–649.

Huang, H. C., 2002. Characteristics of earthquake ground motions and the H/V of microtremors in the southwestern part of Taiwan, *Earthquake Eng. Struct. Dyn.* **31**, 1815–1829.

Idriss, I. M., and Sun, J. I., 1992. *User's Manual for SHAKE91*, Center for Geotechnical Modeling, Department of Civil Engineering, University of California, Davis.

JICA and CGS, 2006. *A Study of Seismic Microzoning of the Wilaya of Algiers in the People's Democratic Republic of Algeria, Final Report, Volume 2*, Oyo International Corp. Nippon Koei Co., Ltd.

Karim, K. R., and Yamazaki, F., 2002. Correlation of the JMA instrumental seismic intensity with strong motion parameters. *Earthquake Eng. Struct. Dyn.* **31**, 1191–1212.

Kramer, S. L., 1996. *Geotechnical Earthquake Engineering*, Prentice-Hall, Inc., USA, 653 pp.

Laouami, N., Slimani, N., Bouhadad, Y., Chatelain, J. L., and Nour, A., 2006. Evidence for fault-related directionality and localized site effects from strong motion recordings of the 2003 Boumerdes (Algeria) earthquake: Consequences on damage distribution and the Algerian seismic code, *Soil Dyn. Earthquake Eng.* **26**, 991–1003.

Meghraoui, M., Maouche, S., Chemaa, B., Cakir, Z., Aoudia, A., Harbi, A., Alasset, P. J., Ayadi, A., Bouhadad, Y., and Benhamouda, F., 2004. Coastal uplift and thrust faulting associated with the M_w=6.8 Zemmouri (Algeria) earthquake of 21 May 2003, *Geophys. Res. Lett.* **31**, L19605 doi:

Nakamura, Y., 1989. *A Method for Dynamic Characteristics Estimation of Subsurface Using Microtremor on the Ground Surface*, Quarterly Report of *RTRI 30*, 25–33.

Oliveira, C. S., Roca, A., and Goula, X., 2006, *Assessing and Managing Earthquake Risk: Geo-Scientific and Engineering Knowledge for Earthquake Risk Mitigation—Developments, Tools, Techniques*, Springer, Netherlands, 561 pp.

Ousalem, H., and Bechtoula, H., 2005. Inventory survey of the 2003 Zemmouri (Algeria) earthquake: Case study of Dergana City, *Journal of Advanced Concrete Technology* **3**, 175–183.

Rathje, E. M., Faraj, F., Russell, S., and Bray, J. D., 2004. Empirical relationships for frequency content parameters of earthquake ground motions, *Earthquake Spectra* **20**, 119–144.

Rodriguez, V. H. S., and Midorikawa, S., 2003. Comparison of spectra ratio techniques for estimation of site effects using microtremor data and earthquake motions recorded at the surface and in boreholes, *Earthquake Eng. Struct. Dyn.* **32**, 1691–1714.

SESAME, 2004. *Guidelines for the Implementation of the H/V Spectral Ratio Technique on Ambient Vibrations: Measurements, Processing and Interpretation*, European Research Project WP12. Project No. EVG1-CT-2000–00026, 62 pp.

Shabestari, K. T., and Yamazaki, F., 2001. A proposal of instrumental seismic intensity scale

compatible with MMI evaluated from three-component acceleration records, *Earthquake Spectra* **17**, 711–723.

Shearer, P. M., and Orcutt, J. A., 1987. Surface and near-surface effects on seismic-waves—theory and borehole seismometer results, *Bull. Seismol. Soc. Am.* **77**, 1168–1196.

Wald, D. J., Quitoriano, V., Heaton, T. H., and Kanamori, H., 1999a. Relationships between peak ground acceleration, peak ground velocity and Modified Mercalli Intensity in California, *Earthquake Spectra* **15**, 557–564.

Wald, D. J., Quitoriano, V., Heaton, T. H., Kanamori, H., Scrivner, C. W., and Worden, C. B., 1999b. TriNet ShakeMaps: Rapid generation of instrumental ground motion and intensity maps for earthquakes in Southern California, *Earthquake Spectra* **15**, 537–556.

Wen, K. L., 1994. Nonlinear soil response in ground motion, *Earthquake Eng. Struct. Dyn.* **23**, 599–608.

Wen, K. L., Chang, T. M., Lin, C. M., and Chiang, H. J., 2006. Identification of nonlinear site response using the H/V spectral ratio method, *Terrestrial Atmospheric and Oceanic Sciences* **17**, 533–546.

Wood, H. O., and Neumann, F., 1931. Modified Mercalli Intensity Scale of 1931, *Bull. Seismol. Soc. Am.* **21**, 277–283.

Yamazaki, F., Lu, L., and Katayama, T., 1992. Orientation error estimation of buried seismographs in array observation, *Earthquake Eng. Struct. Dyn.* **21**, 679–694.

Yamazaki, F., and Ansary, M. A., 1997. Horizontal-to-vertical spectrum ratio of earthquake ground motion for site characterization, *Earthquake Eng. Struct. Dyn.* **26**, 671–689.

(Received 1 April 2009; accepted 5 January 2010)